

# UCLA

## UCLA Previously Published Works

### Title

Comparative Analysis of Human Nucleoside Kinase-Based Reporter Systems for PET Imaging

### Permalink

<https://escholarship.org/uc/item/3v9250hq>

### Journal

Molecular Imaging and Biology, 19(1)

### ISSN

1536-1632

### Authors

Lee, Jason T  
Zhang, Hanwen  
Moroz, Maxim A  
[et al.](#)

### Publication Date

2017-02-01

### DOI

10.1007/s11307-016-0981-6

Peer reviewed



Published in final edited form as:

*Mol Imaging Biol.* 2017 February ; 19(1): 100–108. doi:10.1007/s11307-016-0981-6.

## Comparative Analysis of Human Nucleoside Kinase-Based Reporter Systems for PET Imaging

Jason T. Lee<sup>1,2</sup>, Hanwen Zhang<sup>2</sup>, Maxim A. Moroz<sup>2</sup>, Yury Likar<sup>2</sup>, Larissa Shenker<sup>2</sup>, Nikita Sumzin<sup>2</sup>, Jose Lobo<sup>2</sup>, Juan Zurita<sup>2</sup>, Jeffrey Collins<sup>1</sup>, R. Michael van Dam<sup>1</sup>, and Vladimir Ponomarev<sup>2,3,4</sup>

<sup>1</sup>Crump Institute for Molecular Imaging, Department of Molecular and Medical Pharmacology, David Geffen School of Medicine at UCLA, California NanoSystems Institute Rm 2151, 570 Westwood Plaza, Los Angeles, CA, 90095, USA

<sup>2</sup>Department of Radiology, Memorial Sloan Kettering Cancer Center, 1275 York Ave, New York, NY, 10065, USA

<sup>3</sup>Sloan Kettering Institute, Molecular Pharmacology and Chemistry Program, Memorial Sloan Kettering Cancer Center, New York, NY, 10065, USA

<sup>4</sup>Molecular Imaging Laboratory, Department of Radiology, Memorial Sloan Kettering Cancer Center, 1275 York Ave, New York, NY, 10065, USA

### Abstract

**Purpose**—Radionuclide-based reporter gene imaging has the sensitivity to monitor gene- and cell-based therapies in human subjects. Potential immunogenicity of current viral transgenes warrants development of human-based reporter systems. We compared human nucleoside kinase reporters to a panel of nucleoside analogs of FEAU, FMAU, and FIAU, including the first *in vivo* assessment of L-[<sup>18</sup>F]FEAU.

**Procedures**—Human isogenic U87 cell lines were transduced to express different human reporter genes including dCK-R104M/D133A (dCKDM), dCK-R104Q/D133N (dCKep16A), dCK-A100V/R104M/D133A (dCK3M), and TK2-N93D/L109F (TK2DM), and wild-type dCK (dCK) and herpes simplex virus type-1 (HSVTK) reporter gene as references. *In vitro* cell uptake assays were performed with [<sup>18</sup>F]FEAU, L-[<sup>18</sup>F]FEAU, [<sup>14</sup>C]FMAU, L-[<sup>18</sup>F]FMAU, and [<sup>124</sup>I]FIAU. Micro-positron emission tomography/X-ray computed tomography imaging of xenograft-bearing nu/nu mice was conducted with [<sup>18</sup>F]FEAU, L-[<sup>18</sup>F]FEAU, L-[<sup>18</sup>F]FMAU, and [<sup>124</sup>I]FIAU on consecutive days. A cell viability assay was also performed to assess sensitivities to gemcitabine and bromovinyldeoxyuridine (BVdU).

Correspondence to: Vladimir Ponomarev; ponomarv@mskcc.org.

Electronic supplementary material The online version of this article (doi:10.1007/s11307-016-0981-6) contains supplementary material, which is available to authorized users.

#### **Conflict of Interest**

The authors declare that they have no conflict of interest.

#### **Compliance with Ethical Standards**

Imaging Technology Center are supported in part by NIH *In Vivo* Cellular and Molecular Imaging Centers Grant P50 CA086306, NIH Cancer Center Support Grant P30 CA016042, and NIH SPORE Grant P50 CA092131.

**Results**—*In vitro*, dCKep16A and dCKDM with [<sup>18</sup>F]FEAU exhibited the highest sensitivity and selectivity of the human reporters, second only to HSVTK/[<sup>18</sup>F]FEAU. L-[<sup>18</sup>F]FEAU biodistribution in mice was on par with [<sup>18</sup>F]FEAU and L-[<sup>18</sup>F]FMAU. L-[<sup>18</sup>F]FMAU uptake in isogenic xenografts was highest for all human reporter genes. However, [<sup>18</sup>F]FEAU was the most selective of the short half-life reporter probes due to its minimal recognition by human dCK and relative sensitivity, whereas [<sup>124</sup>I]FIAU permitted imaging at a later time point, improving signal-to-background ratio. Of the human reporter genes, dCKep16A consistently outperformed the other tested reporters. Reporter genes of interest increased potency to the nucleoside analog prodrugs gemcitabine and BVdU.

**Conclusions**—We demonstrate that human nucleoside kinase reporter systems vary significantly in their sensitivity and selectivity for *in vivo* imaging. The sufficiently high signal-to-background ratios and enhanced suicide gene potential support clinical translation.

### Keywords

Human reporter gene imaging; Deoxycytidine kinase; Thymidine kinase; [<sup>18</sup>F]FEAU; L-[<sup>18</sup>F]FEAU; L-[<sup>18</sup>F]FMAU; [<sup>14</sup>C]FMAU; [<sup>124</sup>I]FIAU; Gene and cell therapy; Immunotherapy

### Introduction

Radionuclide-based reporter imaging systems have the sensitivity to monitor gene- and cell-based therapies in human [1]. Extensive preclinical studies of the reporter gene Herpes simplex viral thymidine kinase 1 (HSVTK) and its variants describe the likelihood for longitudinal imaging and clinical translation using clinically available reporter probes [1–7]. Most recently, HSVTK with the F-18 radiolabeled 9-[4-[<sup>18</sup>F]fluoro-3-(hydroxymethyl)butyl]guanine ([<sup>18</sup>F]FHBG) detected localization of adoptively transferred cytotoxic T lymphocytes in a glioma patient [8]. Ongoing clinical trials at Memorial Sloan Kettering Cancer Center and other institutes further support reporter gene imaging as a promising technology for monitoring gene and cell-based therapies [9].

Current developments seek to circumvent the potential immunogenicity of the viral reporter transgenes by designing human-based reporter systems. Sources of human reporter genes include nucleoside kinases, dopamine receptor, somatostatin receptor, norepinephrine transporter, and sodium iodide symporter. Nucleoside kinases are particularly attractive because their phosphorylation of substrates permits signal amplification and trapping. Select mutations at the active site of human deoxycytidine kinase (dCK) [10–12] and thymidine kinase (TK) [13, 14] have expanded their repertoire of nucleoside substrates with properties potentially also amenable to reporter gene imaging. Additionally, several nucleoside analog probes have been developed for reporter imaging including [<sup>18</sup>F]labeled [<sup>18</sup>F]FHBG, 2'-deoxy-2'-[<sup>18</sup>F]fluoro-5-ethyl-1-β-D-arabinofuranosyluracil ([<sup>18</sup>F]FEAU), 1-(2-deoxy-2'-[<sup>18</sup>F]fluoro-β-L-arabinofuranosyl)-5-methyluracil (L-[<sup>18</sup>F]FMAU), and I-124 labeled 2'-deoxy-2'-fluoro-5-[<sup>124</sup>I] iodo-1-β-D-arabinofuranosyluracil ([<sup>124</sup>I]FIAU) [1, 14]. We previously described a deoxycytidine kinase mutant (dCKDM) with specificity for pyrimidine analogs including [<sup>18</sup>F]FEAU. We successfully demonstrated the ability of dCKDM and [<sup>18</sup>F]FEAU to monitor chimeric antigen receptor-based adoptive immunotherapy *in vivo* by positron emission tomography (PET) [15]. More recently, the

probe L-[<sup>18</sup>F]FMAU was applied to two novel reporter gene mutants, hTK2-N93D/L109F (TK2DM) and dCKA100VTM (dCK3M), with normalized sensitivities at least comparable to the mutant HSVTKsr39/[<sup>18</sup>F]FHBG reporter imaging system [14, 16]. The latter was further evaluated for long-term PET monitoring of mouse and human hematopoietic stem cell engraftment and reported no differential effects on cell cycle, lineage distribution, or cell trafficking [16].

Some nucleoside-based reporter genes may have the added benefit of suicide gene potential. This provides a mechanism for elimination of rogue reporter gene-expressing cells with clinically approved nucleoside analog chemotherapeutics such as gemcitabine and bromovinyldeoxyuridine (BVdU) [15]. Additionally, reporter genes may be more promiscuous than their natural mammalian counterparts for certain therapeutic derivatives of nucleosides, thus potentially lowering toxicity to normal organs [17]. The assessment of reporter gene systems should include characterization of reporter genes for enhanced sensitivity to clinically relevant therapeutics.

Here, we compared several of these previously developed mutant variants of human WT dCK (here referred to as dCK) and WT TK2 (here referred to as TK2) reporter genes that have the ability to phosphorylate thymidine against a panel of radiolabeled thymidine analogs. We sought to determine the optimal enzymatic reporter gene/reporter probe combination based on four criteria: (1) biodistribution and clearance, (2) sensitivity, (3) selectivity, and (4) enhanced suicide gene potential.

## Materials and Methods

### Cell Lines, FACS, and Western Blot Analyses

U87 cell lines were cultured at 5 % CO<sub>2</sub> and 37 °C in MEM media, supplemented with 10 % FBS and 2 mM L-glutamine. Generation of isogenic cell lines from parental U87 cells (here referred to as WT) bearing dCK, dCK-R104M/D133A (dCKDM) [9, 10], dCK-R104Q/D133N (dCKep16A) [11], dCK-A100V/R104M/D133A (dCK3M) [10, 11], TK2-N93D/L109F (TK2DM) [14], and HSVTK reporter genes fused to the green fluorescent protein (GFP) were described previously [15]. SFG-based helper-free retroviruses encoding each of the mutant genes were produced by transient transfection of H29 producer cells. U87 cells were incubated with virus media with 2 µg/mL polybrene for 24 h. Fluorescence-activated cell sorting was employed to select comparable population distributions of GFP-expressing cells across all isogenic cell lines. Western blot analysis was performed as described previously [15]. Proteins were detected using mouse monoclonal antibody specific for GFP (clone 7.1, Roche) and antihuman β-actin polyclonal antibody (Abcam).

### Radiolabeled Probes

Preparations of [<sup>18</sup>F]FEAU and [<sup>124</sup>I]FIAU were described previously [18]. L-[<sup>18</sup>F]FEAU was synthesized according to the protocol for [<sup>18</sup>F]FEAU, except using the starting precursor (2-*O*-[(trifluoromethyl)sulfonyl]-1,3,5-tri-*O*-benzoyl-α-L-ribofuranose instead of 2-*O*-[(trifluoromethyl)sulfonyl]-1,3,5-tri-*O*-benzoyl-α-D-ribofuranose). The L-[<sup>18</sup>F]FEAU synthesis protocol was adopted for the synthesis of L-[<sup>18</sup>F]FMAU by using 5-

methyl-uracil to react with 2-deoxy-2- $^{18}\text{F}$ fluoro-1,3,5-tri-*O*-benzoyl- $\alpha$ -L-arabinofuranose. The radiochemical purities of all probes were >99 %, and the specific activities were >555 GBq/mmol. 2- $^{14}\text{C}$ 1-(2'-Fluoro-2'-deoxy-D-arabinofuranosyl)-5-methyluracil ( $^{14}\text{C}$ FMAU) was obtained from Moravek Biochemicals (2 GBq/mmol, MC2041, Moravek Biochemicals).

### In Vitro Uptake Assays of $^{18}\text{F}$ FEAU, L- $^{18}\text{F}$ FEAU, $^{14}\text{C}$ FMAU, L- $^{18}\text{F}$ FMAU, and $^{124}\text{I}$ FIAU

Uptake assays were performed as previously described [15]. Briefly, U87 cells were plated 1 day prior at 50 % confluency in 15-cm tissue culture-treated plates. On the day of the experiment, media was replaced with 15 ml of media conditioned to 37 °C and 5 %  $\text{CO}_2$ , supplemented with 185 kBq/ml F-18 labeled probe, 0.37 kBq/ml  $^{14}\text{C}$ FMAU, or 37 kBq/ml  $^{124}\text{I}$ FIAU and placed in a cell incubator at 37 °C and 5 %  $\text{CO}_2$  for 2 h. Cells were collected by scraping and centrifugation, and washed twice with ice-cold PBS. For F-18 and I-124 labeled assays, cell pellets and corresponding supernatant samples were counted on a Wallac Wizard 3" 1480 Automatic Gamma Counter (PerkinElmer). For  $^{14}\text{C}$ FMAU, cell pellets and supernatant samples were resuspended in Insta-Fluor scintillation liquid (Perkin Elmer), vortexed and counted on a TriCarb 2910 Scintillation Counter (PerkinElmer). Cell pellets were normalized to their respective masses.

### In Vivo microPET/CT Imaging

Animal studies were approved by the MSKCC and UCLA IACUC and were carried out according to the guidelines of the MSKCC Research Animal Resource Center (RARC) and UCLA Division of Laboratory Animal Medicine (DLAM). Nu/nu mice were injected subcutaneously in the left and right flanks with  $2 \times 10^6$  cells resuspended in 50 % phosphate-buffered saline and 50 % Matrigel<sup>TM</sup> (354234, BD Biosciences). Mice underwent microPET/CT imaging approximately 2 weeks after engraftment on consecutive days in the order L- $^{18}\text{F}$ FMAU,  $^{18}\text{F}$ FEAU, and L- $^{18}\text{F}$ FEAU at 2 h or  $^{18}\text{F}$ FEAU and  $^{124}\text{I}$ FIAU at 2 and 24 h postinjection (Inveon PET/CT, Siemens Medical Solutions USA, Inc.). One day prior to  $^{124}\text{I}$ FIAU injection, Lugol's solution (0.5 mL per 100 mL water) was added to the drinking water to block thyroid uptake of radioiodine. At 2 h (L- $^{18}\text{F}$ FMAU,  $^{18}\text{F}$ FEAU, L- $^{18}\text{F}$ FEAU,  $^{124}\text{I}$ FIAU) or 24 h ( $^{124}\text{I}$ FIAU) postinjection of radiolabeled probe, static microPET images were acquired for 300–600 s with an energy window of 350–650 keV for the fluorine-18 probes and 400–590 keV for the iodine-124 probe, followed by 3D histogramming and reconstruction with a zoom factor of 2.1 using 3D-OSEM with two iterations followed by MAP with 18 iterations (beta = 0.1). Images were analyzed using AMIDE version 1.0.5 [19].

### Sensitivity and Selectivity Determination

Two indices were developed to quantitatively evaluate the reporter probe/reporter gene combinations. To compare sensitivities of the reporter systems, a "sensitivity" index was calculated, which accounted for natural cellular uptake in nontransduced WT cells (WT). A "selectivity" index quantified reporter probe uptake due to the reporter gene while also penalizing reporter probes that were substrates for the human dCK enzyme in dCK cells (dCK). To account for interindividual differences, each xenograft uptake was first

normalized to its respective muscle uptake. Sensitivity and selectivity parameters were calculated as follows:

$$\begin{aligned} \text{sensitivity} &= \frac{\text{Reporter}}{\text{WT}} \\ \text{selectivity} &= \frac{\text{Reporter}}{\text{dCK}} \end{aligned}$$

where reporter = U87 reporter gene xenograft uptake, WT = U87 WT xenograft uptake, dCK = U87 dCK xenograft uptake, and units for each variable are in max %ID/g.

## Drugs and IC<sub>50</sub> Assays

Gemcitabine (570287, AK Scientific Inc.) stock solutions were prepared in water. Bromovinyldeoxyuridine (BVdU; B9647, Sigma-Aldrich) was prepared in dimethyl sulfoxide (DMSO). Cells were seeded in 48-well plates ( $1 \times 10^3$  cells/well in 100- $\mu$ l culture media) and allowed to settle for 24 h. Serial drug dilutions (4 $\times$ ) were performed in drug solvent to ensure equal concentrations of solvent for all dilutions and diluted with culture media; 100  $\mu$ l of this dilution was added to cells. Cell viability was analyzed three days later using CellTiter-Glo luminescent cell viability assay. Results were normalized to vehicle control.

## Statistical Analyses

Data are presented as mean  $\pm$  SD. All *p* values were determined with unpaired, two-tailed *t* tests, and values less than 0.05 were considered to be statistically significant. GraphPad Prism 6 software was used to calculate statistics and generate graphs.

## Results

To determine the optimal human reporter system, we generated a panel of isogenic U87 cell lines, each bearing a different reporter gene of interest (Supp Fig. 1a). Western blot analysis of C terminus-fused GFP confirmed the expected reporter protein size (Supp Fig. 1b). Cells were sorted by fluorescence-activated cell sorting (FACS) for GFP to achieve comparable reporter gene expression (Supp Fig. 1c). We conducted *in vitro* uptake assays of five reporter probes to compare four human nucleoside reporter genes: dCK-R104M/D133A (dCKDM), dCK-A100V/R104M/D133A (dCK3M), dCK-R104Q/D133N (dCKep16A), and TK2-N93D/L109F (TK2DM). The five reporter probes are [<sup>18</sup>F]FEAU, L-[<sup>18</sup>F]FMAU, [<sup>14</sup>C]FMAU, [<sup>124</sup>I]FIAU, and the novel L-[<sup>18</sup>F]FEAU. dCKDM and dCKep16A with [<sup>18</sup>F]FEAU exhibited the highest reporter gene-to-WT ratio ( $341 \pm 60$  and  $751 \pm 130$ , respectively) and reporter gene-to-dCK ratio ( $103 \pm 18$  and  $226 \pm 40$ , respectively) for human-based reporters, second only to viral-based HSVTK/[<sup>18</sup>F]FEAU (HSVTK/WT =  $1400 \pm 250$ ; HSVTK/dCK =  $420 \pm 74$ ) (Fig. 1). This was statistically significant compared to the next highest probe, [<sup>124</sup>I]FIAU (reporter gene-to-WT, *p* < 0.001; reporter gene-to-dCK, *p* < 0.001 except TK2DM-to-dCK).

Since the dynamics of gene or cellular therapy may require repeated imaging for monitoring reporter gene expression over time, we compared three different F-18 labeled probes ([<sup>18</sup>F]FEAU, L-[<sup>18</sup>F]FMAU, and L-[<sup>18</sup>F]FEAU) *in vivo*. Immunodeficient nu/nu mice

bearing subcutaneous xenografts were imaged on consecutive days, each day with a different probe. Probe biodistribution 2 h postinjection in normal tissues was largely localized to clearance/secretory tissues (kidneys, bladder, gallbladder, and intestinal tract), with minimal retention in the lung, liver, heart, and skeletal muscle (Fig. 2, Supp Fig. 2). Of the three probes, L-[<sup>18</sup>F]FEAU exhibited the highest intestine ( $12.8 \pm 6.2$  max %ID/g) and lowest skeletal muscle ( $0.511 \pm 0.105$  max %ID/g) tissue uptake. L-[<sup>18</sup>F]FMAU showed lowest overall uptake across the normal tissues.

When human reporter genes dCKDM, dCK3M, and TK2DM were compared in combination with [<sup>18</sup>F]FEAU, L-[<sup>18</sup>F]FEAU, and L-[<sup>18</sup>F]FMAU *in vivo*, both dCKDM and dCK3M with [<sup>18</sup>F]FEAU provided the greatest reporter gene-specific uptake (Fig. 3). L-[<sup>18</sup>F]-FMAU/TK2DM had the highest sensitivity (Fig. 3b). Replacing the methyl with an ethyl group at the 5' position of the L-[<sup>18</sup>F]FMAU nucleobase greatly reduced L-[<sup>18</sup>F]FEAU uptake across all transgene-expressing xenografts. However, after accounting for differences in WT uptake, only TK2DM showed statistical significance between probes, greatest uptake still being with L-[<sup>18</sup>F]FMAU (Fig. 3c,  $p < 0.003$ ). In assessing selectivity, dCK xenografts were compared to WT (Fig. 3d). [<sup>18</sup>F]FEAU uptake in both xenografts was identical and comparable to muscle background, while L-[<sup>18</sup>F]FEAU exhibited nearly 5-fold and L-[<sup>18</sup>F]FMAU, 14-fold ( $p < 0.00001$ ), greater uptake in dCK than WT xenografts. Accounting for dCK uptake, [<sup>18</sup>F]FEAU had the best selectivity across all three probes, namely with dCKDM (maximum 18-fold;  $p < 0.02$  versus L-[<sup>18</sup>F]FEAU;  $p < 0.003$  versus L-[<sup>18</sup>F]FMAU) and dCK3M (maximum 17-fold, not statistically significant). Graphical analysis of sensitivity versus selectivity parameters confirms that [<sup>18</sup>F]FEAU significantly outperforms L-[<sup>18</sup>F]FEAU and L-[<sup>18</sup>F]FMAU in selectivity and maintains comparable sensitivity across all mutant reporter genes. Only TK2DM with L-[<sup>18</sup>F]FMAU or the current standard HSVTK exhibits higher sensitivity (Fig. 3e).

Monitoring adoptively transferred cellular therapies would benefit from imaging longer-lived nuclear reporter probes. Thus, the select reporter genes dCKDM, dCKep16A, and HSVTK were further assessed *in vivo* using [<sup>124</sup>I]FIAU and compared to [<sup>18</sup>F]FEAU (Fig. 4). The 4.18 days half-life of iodine-124 permitted imaging at 2 and 24 h postinjection of [<sup>124</sup>I]FIAU, increasing signal-to-background ratios up to 4-fold at the latter time point. In general, dCKep16A uptake was greater than that of dCKDM with both [<sup>18</sup>F]FEAU at 2 h ( $p < 0.0006$ ) and [<sup>124</sup>I]FIAU at 2 h ( $p < 0.08$ ) and 24 h ( $p < 0.08$ ). While absolute uptake is higher with [<sup>18</sup>F]FEAU at 2 h than with [<sup>124</sup>I]FIAU at 24 h (Fig. 4a, b), the sensitivity and selectivity indices for both probes are comparable (Fig. 4c–e).

Human reporter genes enhanced sensitivity of transduced cells to nucleoside analog prodrugs gemcitabine and BVdU (Fig. 5). Gemcitabine potency was enhanced by at least one order of magnitude in dCK-, dCKDM-, dCK3M-, and dCKep16A-expressing cells, with IC<sub>50</sub> ranging between 0.022 to 0.057 μM, whereas WT did not achieve 50 % inhibition of growth even out to 1 mM (Fig. 5). BVdU exhibited micromolar level potency, but only in cells expressing mutant-dCK reporter genes (IC<sub>50</sub>  $43 \pm 28$ ,  $4.0 \pm 1.1$ , and  $9.4 \pm 3.4$  μM in dCKDM, dCK3M, and dCKep16A, respectively) (Fig. 5). Both results were on par with HSVTK-expressing cells (IC<sub>50</sub>  $0.015 \pm 0.011$  and  $1.7 \pm 1.8$  μM for gemcitabine and BVdU,



respectively). Overexpressing dCK and TK2DM had no effect on sensitivity to BVdU in the concentrations tested up to 1 mM.

## Discussion

Integration of reporter imaging technologies into many currently active clinical protocols could provide a better assessment and understanding of gene- and cell-based therapies. Reporter imaging is particularly applicable to CAR- and TCR-based immunotherapy trials, where real-time monitoring of cell trafficking and efficacy would be critical to patient outcome. HSVTK/<sup>18</sup>F-FHBG-based reporter imaging has successfully detected adoptively transferred therapeutic T cells in a patient with glioma [8]. The continued progress of reporter gene imaging in future clinical trials will depend on the stability of the reporter genes in the body, as well as the sensitivity and selectivity of these systems for detecting target cells. The potential immunogenicity of viral reporter genes has driven the design of human-based reporter mutants. Several human nucleoside kinase orthologs, in combination with various thymidine analog probes, have been developed to address these needs [13–15, 20]. Here, we sought to compare current reporter imaging systems by comparing four parameters: (1) biodistribution and clearance from normal tissues, (2) sensitivity, (3) selectivity, and (4) enhanced suicide gene potential. The latter attribute provides therapeutic potential or possible mechanism for eradication of rogue reporter gene-expressing cells.

### Radiotracer Biodistribution and Reporter Imaging In Vivo

The predominant normal tissue uptakes for [<sup>18</sup>F]FEAU and L-[<sup>18</sup>F]FMAU probes were in the kidneys, urinary bladder, gallbladder, and intestines, indicating significant renal and hepatobiliary excretion. Thus, delayed microPET imaging at later time points may provide enhanced signal-to-background ratios by allowing greater probe elimination. Here, we report the first evaluation of L-[<sup>18</sup>F]FEAU *in vivo* as a potential reporter probe for imaging nucleoside kinase mutant reporters. L-[<sup>18</sup>F]FEAU biodistribution localized to clearance and abdominal tissues slightly higher than [<sup>18</sup>F]FEAU and L-[<sup>18</sup>F]FMAU, suggesting acceptable dosimetry and minimal normal tissue uptake for reporter imaging. Insofar as we have tested, L-[<sup>18</sup>F]FEAU has no advantages over [<sup>18</sup>F]FEAU as a reporter probe, but L-[<sup>18</sup>F]FEAU suffers from increased activity by dCK.

### dCKep16A as an Improved PET Reporter Gene to dCKDM

Sabini *et al.* mutated positions 100, 104, and 133 in the human dCK active site (dCKDM and dCK3M) and demonstrated the importance of amino acid positions 104 and 133 to expand substrate specificity of dCK [10]. Using site-directed mutagenesis, Iyidogan *et al.* created the double-mutant dCKep16A also with amino acid substitutions in positions 104 and 133, and quantified its enzymatic properties for the four natural nucleoside substrates [11]. We report for the first time the application of dCKep16A as a human PET reporter gene with several established thymidine analog PET probes. dCKep16A outperformed dCKDM when used in combination with either [<sup>18</sup>F]FEAU or [<sup>124</sup>I]FIAU. The mutations at amino acid positions 104 and 133 of dCK confer enhanced pyrimidine activity to both mutants, but dCKep16A exhibits an increased specificity constant for thymidine relative to that of dCKDM [11]. This suggests that these two enzyme active site residues are important in



phosphorylation of thymidine analog probes such as FEAU and FIAU and that improvements in probe metabolism seen by dCKep16A may be due to reduction in unfavorable steric (R104Q) and electrostatic interactions (D133N). These mutation differences marginally improved the potency of dCKep16A for the thymidine analog pro-drug, BVdU, without altering its ability to activate the deoxycytidine analog pro-drug, gemcitabine (dCKep16A and dCKDM are not statistically distinguishable for gemcitabine).

### Sensitivity

The *in vivo* dynamic ranges of these reporter systems were significantly lower than anticipated from the *in vitro* findings. [<sup>18</sup>F]FEAU, [<sup>124</sup>I]FIAU, and L-[<sup>18</sup>F]FEAU retentions were less pronounced in reporter gene-expressing versus control cells and, overall, an order of magnitude lower than that of L-[<sup>18</sup>F]FMAU. The reduced uptake may be attributable to probe competition with serum nucleosides [17]. Mice serum thymidine concentrations are sufficiently high to reduce uptake of probes, whereas it is absent in cell culture media [21, 22]. Indeed, mutations in amino acids 104 and 133 confer WT dCK with at least an order of magnitude greater efficiency for deoxycytidine and thymidine, likely increasing competition with analog probes [11, 12]. TK2DM, in contrast, was designed by Campbell *et al.* to exhibit reduced activity for natural nucleosides, thymidine, and deoxycytidine, and with reduced feedback inhibition by thymidine triphosphates [14]. This enhances TK2DM-dependent uptake of L-[<sup>18</sup>F]FMAU above that of TK2 [14], as well as dCK shown here. However, as suggested earlier, the generally high L-[<sup>18</sup>F]FMAU retention in dCK and mutant reporter versus WT cells compared with [<sup>18</sup>F]FEAU and L-[<sup>18</sup>F]FEAU indicates that a substantial proportion of L-[<sup>18</sup>F]FMAU signal is due to reporter gene overexpression independent of the mutations. It would be of interest to confirm these findings with other *in vivo* reporter gene comparison systems [20].

The minimal uptake of these nucleoside analog reporter probes in wild-type nontransduced U87 cells is due in part to the low natural expression of dCK [15]. In contrast, rapidly cycling cells, such as lymphocytes, upregulate dCK substantially upon activation [23]. It is possible that FEAU and FIAU insensitivity to endogenous nucleoside kinases along with optimizations to reduce the activity of the mutant dCK reporter gene for natural nucleosides may substantially expand the dynamic range of this reporter system and its utility for human-based reporter imaging in the clinic.

### Selectivity

Alterations of human dCK at the Arg104 and Asp133 residues endow dCK with the ability to phosphorylate both D- and L-forms of thymidine and deoxyuridine by reducing charge repulsion and steric constraints [12]. Unlike wild-type dCK, the enlarged cavity of these dCK mutants allows acceptance of bulkier 5' groups, such as an ethyl or iodine in the case of FEAU or FIAU, respectively, without reducing the enzyme's observed rate ( $k_{obs}$ ) [15]. This is confirmed in the enhanced *in vitro* uptake of [<sup>18</sup>F]FEAU, L-[<sup>18</sup>F]FEAU, and [<sup>124</sup>I]FIAU in dCKDM-, dCK3M-, and dCKep16A-, but not dCK-overexpressing cell lines. In contrast, we observed [<sup>18</sup>F]FMAU and L-[<sup>18</sup>F]FMAU, which differ from [<sup>18</sup>F]FEAU, [<sup>124</sup>I]FIAU, and L-[<sup>18</sup>F]FEAU at the 5' methyl, to be substrates for dCK *in vitro*. This is not unexpected as both methyl compounds were reported substrates for endogenous nucleoside

kinases [24]. In fact, both probes were suggested to be useful agents for imaging cellular proliferation and cellular stress *in vivo* [24, 25]. As a reporter imaging probe, L-[<sup>18</sup>F]FMAU's recognition by dCK proves to be a challenge in certain applications. For example, it would be difficult to discriminate reporter gene-bearing, adoptively transferred lymphocytes that have infiltrated highly proliferative tumors. The *in vivo* enumeration of therapeutic lymphocytes may also be difficult as activated cells can disproportionately increase signal intensity.

### Potential for [<sup>124</sup>I]FIAU and dCK Mutants

Despite issues with deiodination, [<sup>124</sup>I]FIAU with mutant human dCK may be a promising combination for certain imaging applications. The much longer radioactivity half-life of [<sup>124</sup>I]FIAU (4.18 days) has two advantages. First, it permits imaging on the order of days during which the probe will be cleared from nontarget tissues, including the abdominal regions, whereas [<sup>18</sup>F]FEAU and L-[<sup>18</sup>F]FMAU exhibit generally moderate residual radioactivity in nontarget tissues at 2 h imaging time points. Second, in adoptive cell transfer therapies, cells of interest can be pre-labeled with [<sup>124</sup>I]FIAU *ex vivo* prior to injection. This significantly reduces systemic free iodine-124 and has the added advantage of minimal background because phosphorylated probes cannot readily diffuse out of the cell unless cellular integrity is compromised. In both scenarios, cell trafficking can be followed over the course of days. Results here demonstrate that reporter gene-expressing cells can be discriminated from background when imaging with <sup>124</sup>I-FIAU at 24 h and possibly even later. Currently, [<sup>124</sup>I]FIAU/HSVTK imaging is part of an ongoing immunotherapy clinical trial (clinical trial #NCT01140373, <https://clinicaltrials.gov>) [9]. In order to avert potential immunogenicity of HSVTK, [<sup>124</sup>I]FIAU/dCKep16A may be a favorable alternative reporter imaging system.

### Reporter Gene-Specific Enhancement of Suicidal Activity

Expression of these reporter genes in transduced cells sensitizes them to gemcitabine and BVdU. Gemcitabine was not substantially more potent in U87 cells overexpressing the mutant-dCK reporter genes compared to dCK, confirming previous findings [12]. In contrast, the antiviral BVdU may be a more promising alternative. At the doses tested and nontransduced, dCK or TK2DM cells were insensitive to BVdU. Its potency was higher in cells expressing dCK mutant reporter genes compared to overexpression of dCK and to WT cells. Furthermore, BVdU is reported to be a selective inhibitor of particular viral TKs and is generally well tolerated in humans. BVdU is approved for use in Europe as an antiviral therapy [26].

### Conclusions

Reporter imaging technologies are anticipated to contribute significantly to the monitoring of gene and cell-based therapies. Continued improvements in sensitivity and selectivity of these technologies will be beneficial. Towards this end, we report here an overall more sensitive and selective human reporter gene, dCKep16A. Further studies should characterize the mutant-dCK reporter genes and, in particular, the promising dCKep16A, for their efficiency at metabolizing endogenous nucleoside substrates and their kinetics with different

reporter probes. Reducing mutant reporter gene activity for natural substrates, while maintaining or even enhancing high specificity for reporter probes such as [<sup>18</sup>F]FEAU and [<sup>124</sup>I]FIAU, would greatly expand their dynamic ranges. [<sup>18</sup>F]FEAU was previously shown to be a poor substrate for human TK1, TK2, and here, dCK, thereby further improving selectivity [17]. Additionally, reporter probe accessibility to target cells such as tissue penetrance and transport across cell membranes must also be considered. Immunogenicity and biological half-life dynamics should be characterized, the latter important for imaging transcriptional gene regulation involving inducible promoters such as for longitudinal monitoring of T cell activation [27].

Current focus on human-based reporter imaging systems is of particular interest to circumvent potential reporter transgene immunogenicity. The human mutant-dCK reporter gene, dCKep16A, in combination with [<sup>18</sup>F]FEAU or [<sup>124</sup>I]FIAU is a highly promising reporter system given its relative sensitivity, high selectivity, and enhanced suicide gene potential.

## Supplementary Material

Refer to Web version on PubMed Central for supplementary material.

## Acknowledgments

We thank Dr. Caius G. Radu at the Ahmanson Translational Imaging Division at UCLA for donating the pMSCV-hTK2 plasmid. We thank Dr. Pat Zanzonico and Valerie Longo at Memorial Sloan Kettering Cancer Center (MSKCC) and Waldemar Ladno and Dr. Olga Sergeeva at the UCLA Crump Institute for Molecular Imaging for their imaging technical assistance and expertise. We thank Eva M. Burnazi at MSKCC for her radiochemistry technical expertise. We thank Dr. Ronald Blasberg for his help in preparing this manuscript. Technical services were provided by the MSKCC Small Animal Imaging Core Facility and the UCLA Crump Institute's Preclinical Imaging Technology Center.

### *Funding*

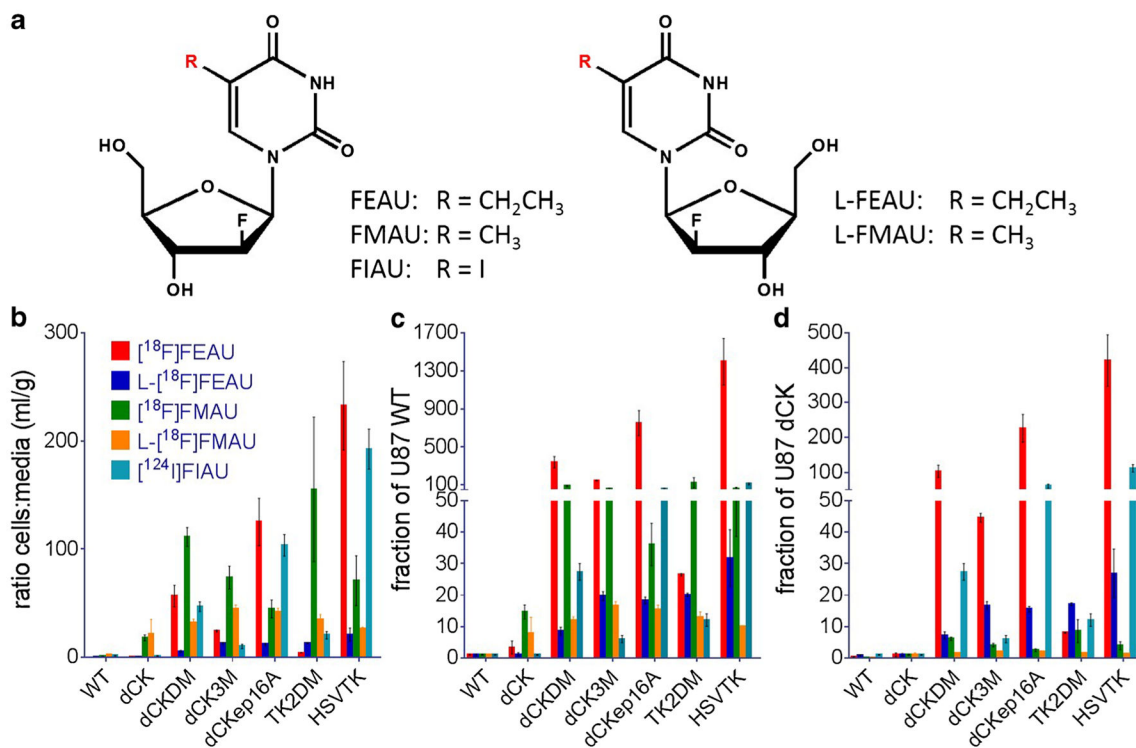
This work was supported by the Molecular Imaging: Training for Oncology (MITO) of the National Institutes of Health, Cancer Education and Career Development Program 5R25CA096945-09 grant, NIH P50 CA86438-11, R01 CA161138, and R01 CA163980 grants. Technical services provided by the MSKCC Small-Animal Imaging Core Facility are supported in part by NIH Small-Animal Imaging Research Program (SAIRP), NIH Shared Instrumentation Grant No 1 S10 RR020892-01, NIH Shared Instrumentation Grant No 1 S10 RR028889-01, and NIH Center Grant P30 CA08748. Technical services provided by the UCLA Crump Institute's Preclinical

## References

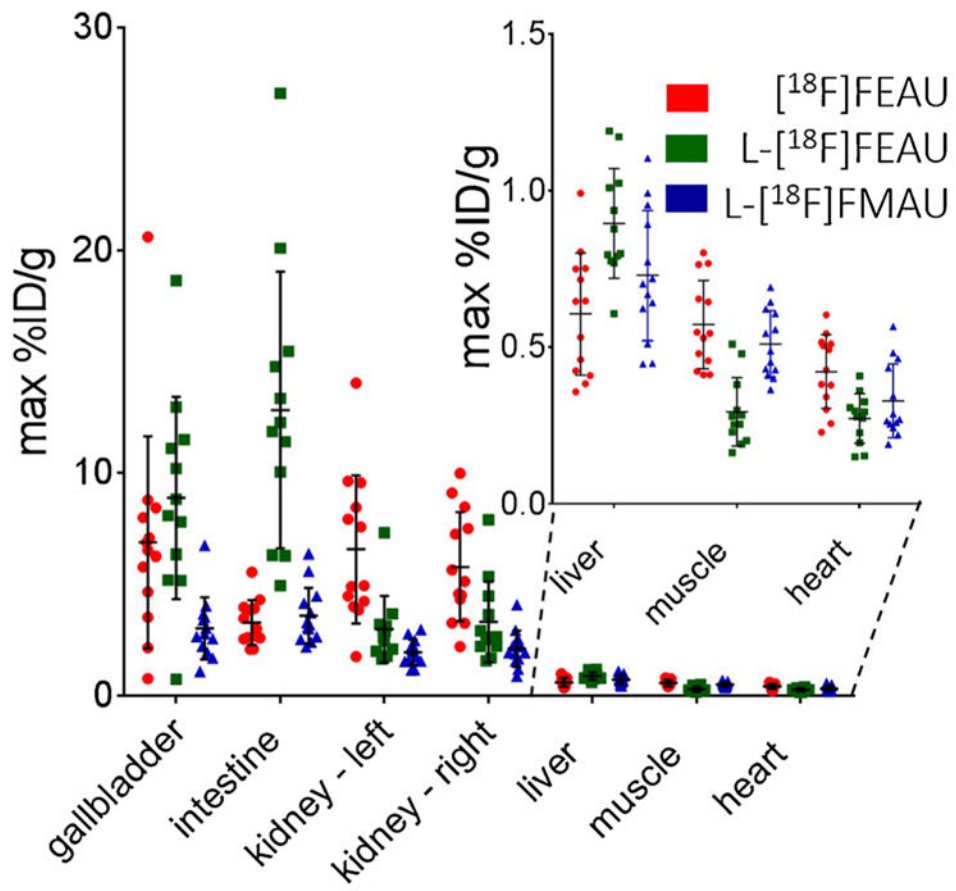
1. Brader P, Serganova I, Blasberg RG. Noninvasive molecular imaging using reporter genes. *J Nucl Med: Off Publ Soc Nucl Med.* 2013; 54:167–172.
2. Koehne G, Doubrovin M, Doubrovina E, et al. Serial *in vivo* imaging of the targeted migration of human HSV-TK-transduced antigen-specific lymphocytes. *Nat Biotechnol.* 2003; 21:405–413. [PubMed: 12652311]
3. Likar Y, Dobrenkov K, Olszewska M, et al. A new acycloguanosine-specific supermutant of herpes simplex virus type 1 thymidine kinase suitable for PET imaging and suicide gene therapy for potential use in patients treated with pyrimidine-based cytotoxic drugs. *J Nucl Med : Off Publ Soc Nucl Med.* 2008; 49:713–720.
4. Gambhir SS, Bauer E, Black ME, et al. A mutant herpes simplex virus type 1 thymidine kinase reporter gene shows improved sensitivity for imaging reporter gene expression with positron emission tomography. *Proc Natl Acad Sci U S A.* 2000; 97:2785–2790. [PubMed: 10716999]

5. Yaghoubi SS, Gambhir SS. PET imaging of herpes simplex virus type 1 thymidine kinase (HSV1-tk) or mutant HSV1-sr39tk reporter gene expression in mice and humans using [18F]FHBG. *Nat Protoc.* 2006; 1:3069–3075. [PubMed: 17406570]
6. Miyagawa T, Gogiberidze G, Serganova I, et al. Imaging of HSV-tk Reporter gene expression: comparison between [18F]FEAU, [18F]FFEAU, and other imaging probes. *J Nucl Med: Off Publ Soc Nucl Med.* 2008; 49:637–648.
7. Su H, Chang DS, Gambhir SS, Braun J. Monitoring the antitumor response of naive and memory CD8 T cells in RAG1<sup>-/-</sup> mice by positron-emission tomography. *J Immunol.* 2006; 176:4459–4467. [PubMed: 16547284]
8. Yaghoubi SS, Jensen MC, Satyamurthy N, et al. Noninvasive detection of therapeutic cytolytic T cells with 18F-FHBG PET in a patient with glioma. *Nat Clin Pract Oncol.* 2009; 6:53–58. [PubMed: 19015650]
9. Slovin SF, Wang X, Hullings M, et al. Chimeric antigen receptor (CAR<sup>+</sup>) modified T cells targeting prostate-specific membrane antigen (PSMA) in patients (pts) with castrate metastatic prostate cancer (CMPC). *ASCO Meet Abstr.* 2013; 31:72.
10. Sabini E, Ort S, Monnerjahn C, Konrad M, Lavie A. Structure of human dCK suggests strategies to improve anticancer and antiviral therapy. *Nat Struct Biol.* 2003; 10:513–519. [PubMed: 12808445]
11. Iyidogan P, Lutz S. Systematic exploration of active site mutations on human deoxycytidine kinase substrate specificity. *Biochemistry.* 2008; 47:4711–4720. [PubMed: 18361501]
12. Hazra S, Ort S, Konrad M, Lavie A. Structural and kinetic characterization of human deoxycytidine kinase variants able to phosphorylate 5-substituted deoxycytidine and thymidine analogues. *Biochemistry.* 2010; 49:6784–6790. [PubMed: 20614893]
13. Ponomarev V, Doubrovin M, Shavrin A, et al. A human-derived reporter gene for noninvasive imaging in humans: mitochondrial thymidine kinase type 2. *J Nucl Med: Off Publ Soc Nucl Med.* 2007; 48:819–826.
14. Campbell DO, Yaghoubi SS, Su Y, et al. Structure-guided engineering of human thymidine kinase 2 as a positron emission tomography reporter gene for enhanced phosphorylation of non-natural thymidine analog reporter probe. *J Biol Chem.* 2012; 287:446–454. [PubMed: 22074768]
15. Likar Y, Zurita J, Dobrenkov K, et al. A new pyrimidine-specific reporter gene: a mutated human deoxycytidine kinase suitable for PET during treatment with acycloguanosine-based cytotoxic drugs. *J Nucl Med: Off Publ Soc Nucl Med.* 2010; 51:1395–1403.
16. McCracken MN, Gschweng EH, Nair-Gill E, et al. Long-term *in vivo* monitoring of mouse and human hematopoietic stem cell engraftment with a human positron emission tomography reporter gene. *Proc Natl Acad Sci U S A.* 2013; 110:1857–1862. [PubMed: 23319634]
17. Chung, J-K., Kang, J., Kang, K. Reporter Gene Imaging with PET/ SPECT. In: Gambhir, SS., editor. *Molecular Imaging with Reporter Genes.* Cambridge University Press; Cambridge: 2010. p. 70-87.
18. Zhang H, Cantorias MV, Pillarsetty N, Burnazi EM, Cai S, Lewis JS. An improved strategy for the synthesis of [(1)(8)F]-labeled arabinofuranosyl nucleosides. *Nucl Med Biol.* 2012; 39:1182–1188. [PubMed: 22819195]
19. Loening AM, Gambhir SS. AMIDE: a free software tool for multimodality medical image analysis. *Mol Imaging.* 2003; 2:131–137. [PubMed: 14649056]
20. Gil JS, Machado HB, Campbell DO, et al. Application of a rapid, simple, and accurate adenovirus-based method to compare PET reporter gene/PET reporter probe systems. *Mol Imaging Biol: MIB: Off Publ Acad Mol Imaging.* 2013; 15:273–281.
21. Tseng JR, Dandekar M, Subbarayan M, et al. Reproducibility of 3'-deoxy-3'-(18)F-fluorothymidine microPET studies in tumor xenografts in mice. *J Nucl Med: Off Publ Soc Nucl Med.* 2005; 46:1851–1857.
22. Lee DJ, Prenskey W, Krause G, Hughes WL. Blood thymidine level and iododeoxyuridine incorporation and reutilization in DNA in mice given long-acting thymidine pellets. *Cancer Res.* 1976; 36:4577–4583. [PubMed: 1000502]
23. Radu CG, Shu CJ, Nair-Gill E, et al. Molecular imaging of lymphoid organs and immune activation by positron emission tomography with a new [18F]-labeled 2'-deoxycytidine analog. *Nat Med.* 2008; 14:783–788. [PubMed: 18542051]

24. Nishii R, Volgin AY, Mawlawi O, et al. Evaluation of 2'-deoxy-2'-[18F]fluoro-5-methyl-1-beta-L: -arabinofuranosyluracil ([18F]-L: -FMAU) as a PET imaging agent for cellular proliferation: comparison with [18F]-D: -FMAU and [18F]FLT. *Eur J Nucl Med Mol Imaging*. 2008; 35:990–998. [PubMed: 18057932]
25. Tehrani OS, Douglas KA, Lawhorn-Crews JM, Shields AF. Tracking cellular stress with labeled FMAU reflects changes in mitochondrial TK2. *Eur J Nucl Med Mol Imaging*. 2008; 35:1480–1488. [PubMed: 18265975]
26. De Clercq E. Discovery and development of BVDU (brivudin) as a therapeutic for the treatment of herpes zoster. *Biochem Pharmacol*. 2004; 68:2301–2315. [PubMed: 15548377]
27. Ponomarev V, Doubrovin M, Lyddane C, et al. Imaging TCR-dependent NFAT-mediated T-cell activation with positron emission tomography *in vivo*. *Neoplasia*. 2001; 3:480–488. [PubMed: 11774030]

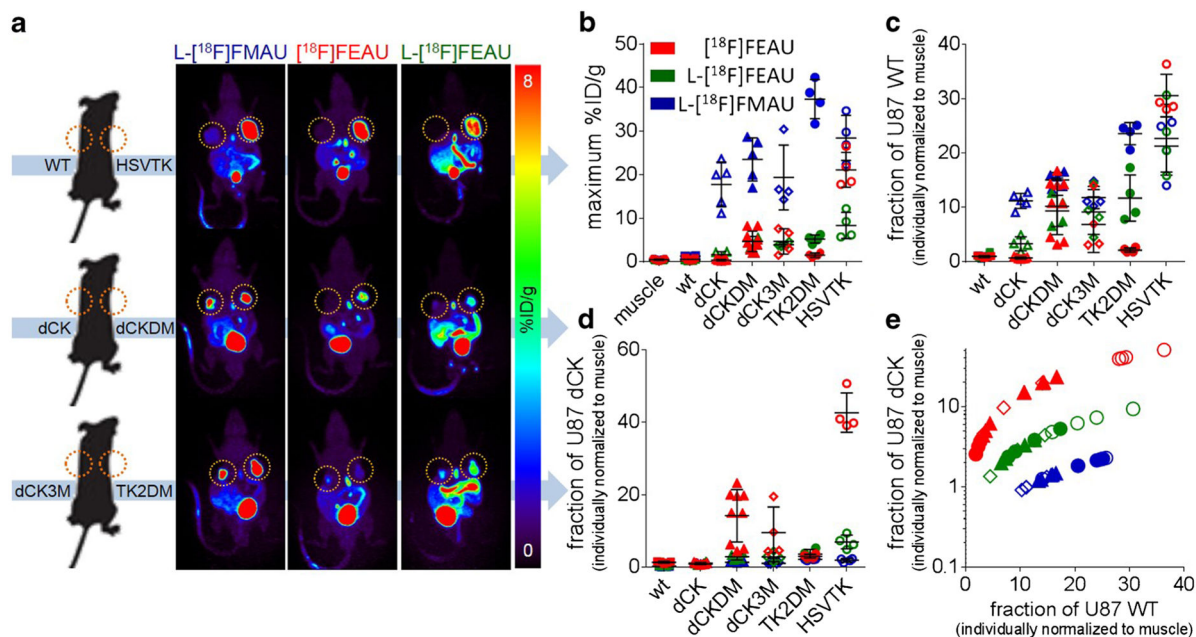
**Fig. 1.**

*In vitro* uptake in isogenic U87 reporter cell lines across a panel of radiolabeled nucleoside analog probes. **a** Structures of reporter probes used in this study. Uptake data presented **b** as cell activity normalized to supernatant media activity, **c** as fraction of U87 WT uptake, and **d** as fraction of U87 dCK uptake. All cell lines were derived from the parental U87 WT, and the term “U87” is omitted for simplicity.

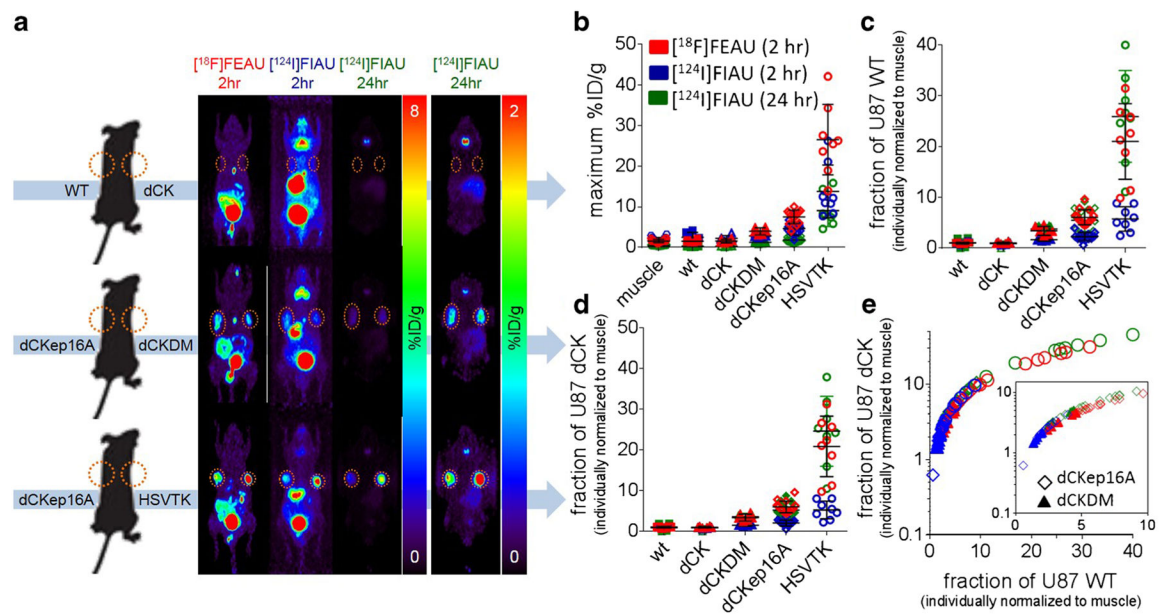


**Fig. 2.**  
Biodistribution of thymidine analog reporter probes by microPET ROI analysis



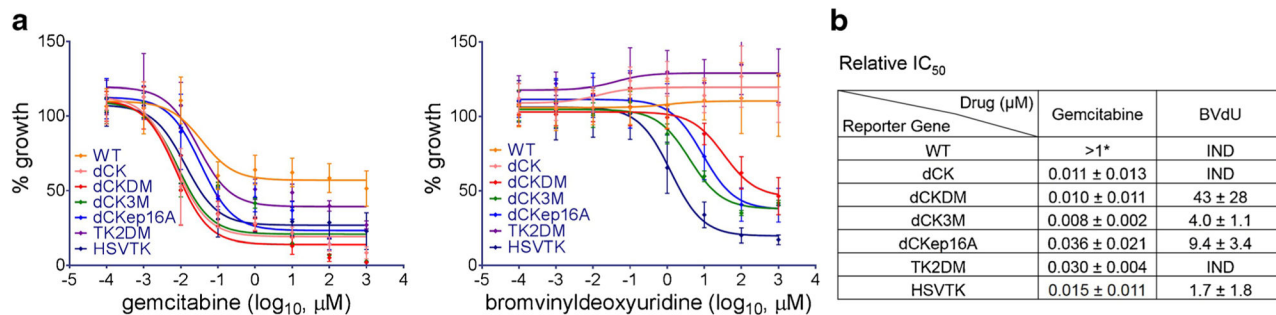
**Fig. 3.**

*In vivo* comparisons of fluorine-18 nucleoside reporter probes. **a** Representative maximum intensity projection microPET images of nu/nu mice with established subcutaneous xenografts of isogenic U77 reporter cell lines and L-[<sup>18</sup>F]FMAU, [<sup>18</sup>F]FEAU, and L-[<sup>18</sup>F]FEAU. The same mouse was imaged on three consecutive days with the reporter probes L-[<sup>18</sup>F]FMAU, [<sup>18</sup>F]FEAU, and L-[<sup>18</sup>F]FEAU, respectively. Xenografts are delineated by broken circles. microPET region-of-interest analysis presented **b** as maximum percent injected dose per gram (%ID/g), **c** as fraction of U87 WT uptake after intra-individual normalization to muscle uptake, and **d** as fraction of U87 dCK uptake after intra-individual normalization to muscle uptake. **e** Reporter system comparisons based on calculated sensitivity and selectivity indices from microPET imaging.



**Fig. 4.**

*In vivo* comparisons of [ $^{18}\text{F}$ ]FEAU and [ $^{124}\text{I}$ ]FIAU. **a** Representative maximum intensity projection microPET images of nu/nu mice with established subcutaneous xenografts of isogenic U87 reporter cell lines and [ $^{18}\text{F}$ ]FEAU at 2 h and [ $^{124}\text{I}$ ]FIAU at 2 and 24 h. The same mouse was imaged on three consecutive days with the reporter probes [ $^{18}\text{F}$ ]FEAU and [ $^{124}\text{I}$ ]FIAU. Xenografts are delineated by *broken circles*. microPET region-of-interest analysis presented **b** as maximum percent injected dose per gram (%ID/g), **c** as fraction of U87 WT uptake after intra-individual normalization to muscle uptake, and **d** as fraction of U87 dCK uptake after intra-individual normalization to muscle uptake. **e** Reporter system comparisons based on calculated sensitivity and selectivity indices from microPET imaging. *Inset graph* shows only dCKDM and dCKep16A.

**Fig. 5.**

Suicide gene potential of reporter mutants with clinically-relevant prodrugs. Sensitivities to two clinically-relevant nucleoside analog prodrugs, gemcitabine and bromovinyldeoxyuridine (BVdU), were assessed across the isogenic U87 cell lines. **a** Representative dose-response curves for **a** gemcitabine and **b** BVdU. **c** Calculated relative IC<sub>50</sub> values for each drug. Never reached 50 % of control (*asterisk*). *IND* IC<sub>50</sub> was indeterminate.